

The Quark Structure of Light Mesons

B. C. Metsch, H. R. Petry

Institut für Theoretische Kernphysik,

Universität Bonn, Nußallee 14-16, 53115 Bonn, Germany

E-mail: metsch@itkp.uni-bonn.de

TK-96-25 29.06.1996

1 Introduction

A glance at the experimental spectra of light mesons reveals two general trends each with a conspicuous exception:

- In general states that can be attributed to the same orbital angular momentum multiplets show only small spin-orbit splittings. Examples are $f_1(1285)$ and $f_2(1270)$, $a_3(2050)$ and $a_4(2040)$, $K_2(1770)$ and $K_3^*(1780)$. Notable exceptions are the low positions of the $f_0(980)$ and $a_0(980)$.
- For every isovector state there is energetically degenerate an isoscalar partner. The best known example is of course $\rho(770)$ and $\omega(782)$, but also $h_1(1170)$ and $b_1(1235)$ and many other pairs, up to $a_6(2450)$ and $f_6(2510)$. This is of course nothing but the well known fact that the inter-quark forces are flavor symmetric. Note however, that this rule does *not* apply to the pseudoscalar mesons π, η, η' , which exhibit a mass splitting as large as any in the meson spectrum.

Any model of hadrons should address these observations. This seems to be especially important for the identification of exotic mesonic states, like hybrids, dimesonic states or the appreciation of the predictions on glueballs from lattice-QCD [1]. The most successful framework for a coherent description of both meson and baryon spectra certainly is the non-relativistic quark model. Here, the basic assumptions are that the excitations of hadrons can be effectively described by constituent quarks, that interact via potentials in the framework of the Schrödinger equation. A particular version of the NRQM implementing confinement via a linear potential in the spirit of the string model and substituting the widely used Fermi-Breit interaction by an instanton induced effective quark interaction, can simultaneously describe meson and baryon masses up-to excitation energies of roughly 1 GeV [2]. In this framework the masses of the bulk of mesons are determined by the confinement potential alone, thus avoiding unwanted spin-orbit splittings. The instanton induced force selectively acts only on pseudoscalar states and accounts for the large π, η, η' splitting and mixing of isoscalars. However, it should be pointed out that this treatment can be critizised at two points at least:

- Binding energies (especially of the ground state mesons) are too large compared to the constituent masses to justify a non-relativistic treatment;
- The Schrödinger wave functions are incorrect at large energies and/or momentum transfers.

Although these seem to be rather formal objections they do matter in practice. Let us consider the calculation of some electro-weak decay observables for light mesons as gathered in Table 1 [3]:

Table 1: Comparison of experimental and calculated electro-weak meson decay observables for the relativistic quark model 'RQM' and non-relativistic results 'NRQM'.

Decay	exp. [30]	RQM	NRQM
f_π [MeV]	131.7 ± 0.2	130	1440
f_K [MeV]	160.6 ± 1.4	180	730
$\Gamma(\pi^0 \rightarrow \gamma\gamma)$ [eV]	7.8 ± 0.5	7.6	30000
$\Gamma(\eta \rightarrow \gamma\gamma)$ [eV]	460 ± 5	440	18500
$\Gamma(\eta' \rightarrow \gamma\gamma)$ [eV]	4510 ± 260	2900	750
$\Gamma(\rho \rightarrow e^+e^-)$ [keV]	6.8 ± 0.3	6.8	8.95
$\Gamma(\omega \rightarrow e^+e^-)$ [keV]	0.60 ± 0.02	0.73	0.96
$\Gamma(\phi \rightarrow e^+e^-)$ [keV]	1.37 ± 0.05	1.24	2.06

Although the dilepton decays of the vector mesons can be more or less accounted for non-relativistically, the discrepancies for the weak decay constants amount up to an order of magnitude and the calculated values for the $\gamma\gamma$ -decay are beyond discussion. The agreement with data can be drastically improved in a relativistically covariant quark model we developed on the basis of the Bethe–Salpeter equation, see section 2. In section 3 we will present some results for spectra, electro-weak decays and form factors in this model. In section 4 we will demonstrate that in contrast to the non-relativistic model the instanton induced interaction not only acts on pseudoscalar mesons but also determines the structure and splittings of scalar mesons. Here we will touch upon the consequences in particular for the possible interpretation of the newly discovered $f_0(1500)$ resonance as a glueball, see also [15]. The last section contains some conclusions and an outlook.

2 A relativistic quark model

In momentum space the Bethe–Salpeter equation for the amplitude

$$[\chi_P(x)]_{\alpha\beta} = \left\langle 0 \left| T \Psi_\alpha^1\left(\frac{1}{2}x\right) \bar{\Psi}_\beta^2\left(-\frac{1}{2}x\right) \right| P \right\rangle, \quad (1)$$

reads [5, 4]:

$$\chi_P(p) = S_1^F(p_1) \int \frac{d^4 p'}{(2\pi)^4} [-i K(P, p, p') \chi_P(p')] S_2^F(-p_2) \quad (2)$$

where $p_1 = \frac{1}{2}P + p$, $p_2 = \frac{1}{2}P - p$ denote the momenta of the quark and antiquark respectively, P is the four momentum of the bound state and S^F and K are the Feynman quark propagators and the irreducible quark interaction kernel.

We will construct the relativistic quark model very similar to the non relativistic potential model. Therefore both S_F and K are given by a phenomenological (but formally covariant) *Ansatz* as follows:

- The propagators are assumed to be of the free form $S_i^F(p) = i/(p - m_i + i\epsilon)$, with an effective constituent-quark mass m_i ;
- It is assumed that the interaction kernel only depends on the components of p and p' perpendicular to P , i.e. $K(P, p, p') = V(p_{\perp P}, p'_{\perp P})$ with $p_{\perp P} := p - (pP/P^2)P$.

Integrating in the bound state rest frame over the time component and introducing the equal-time (or Salpeter) amplitude

$$\Phi(\vec{p}) := \int dp^0 \chi_P(p^0, \vec{p}) \Big|_{P=(M, \vec{0})} = \int dp_{||P} \chi_P(p_{||P}, p_{\perp P}) \Big|_{P=(M, \vec{0})} \quad (3)$$

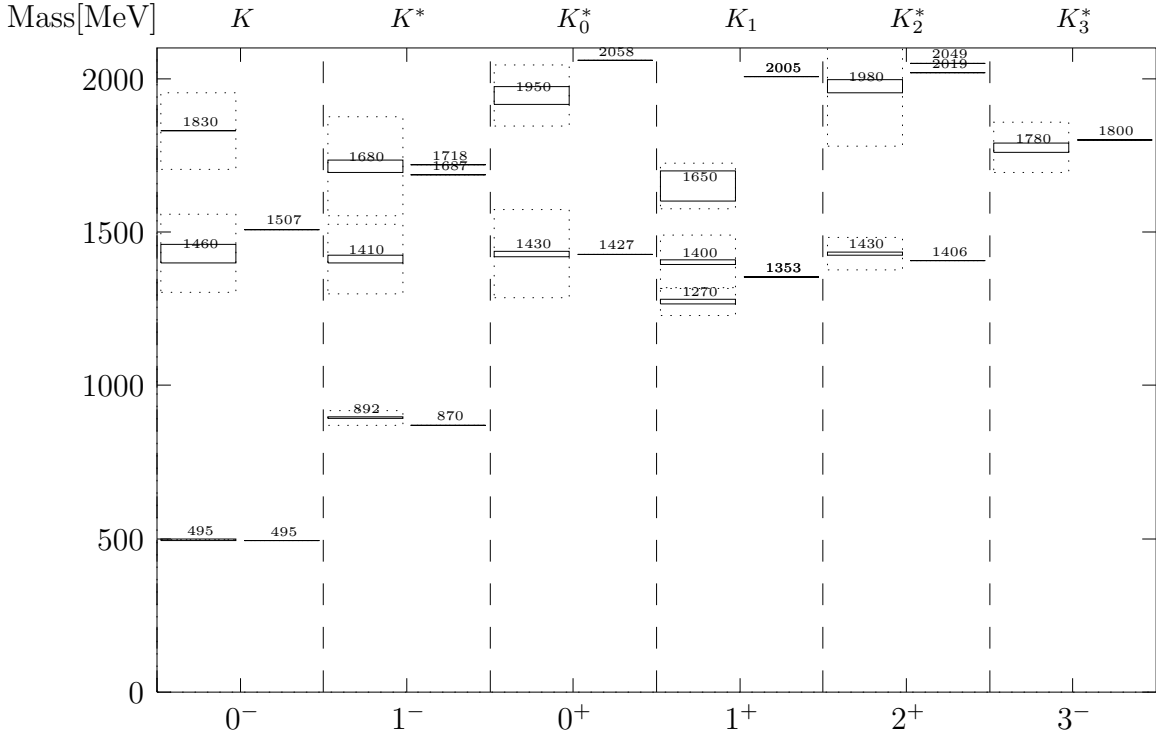


Figure 1: Strange meson spectrum. In the left part of each column the experimental resonance position [30] and its error is indicated by a rectangle, the total decay width is given by a dotted rectangle; the lines in the right part of each column represent the calculated masses.

we thus arrive at the well-known Salpeter equation [6]:

$$\begin{aligned} \Phi(\vec{p}) &= \int \frac{d^3 p'}{(2\pi)^3} \frac{\Lambda_1^-(\vec{p}) \gamma^0 [(V(\vec{p}, \vec{p}')) \Phi(\vec{p}')] \gamma^0 \Lambda_2^+(-\vec{p})}{M + \omega_1 + \omega_2} \\ &- \int \frac{d^3 p'}{(2\pi)^3} \frac{\Lambda_1^+(\vec{p}) \gamma^0 [(V(\vec{p}, \vec{p}')) \Phi(\vec{p}')] \gamma^0 \Lambda_2^-(\vec{p})}{M - \omega_1 - \omega_2} \end{aligned} \quad (4)$$

with the projectors $\Lambda_i^\pm = (\omega_i \pm H_i)/(2\omega_i)$, the Dirac Hamiltonian $H_i(\vec{p}) = \gamma^0(\vec{\gamma}\vec{p} + m_i)$ and $\omega_i = (m_i^2 + \vec{p}^2)^{1/2}$.

The amplitudes Φ have been calculated by solving the Salpeter equation for a kernel including a confining interaction of the form

$$\int d^3 p' [V_C^V(\vec{p}, \vec{p}') \Phi(\vec{p}')] = - \int d^3 p' \mathcal{V}((\vec{p} - \vec{p}')^2) \frac{1}{2} [\gamma^0 \Phi(\vec{p}') \gamma^0 + 1 \Phi(\vec{p}') 1] \quad (5)$$

where the spin structure was chosen such as to minimize spin orbit effects. In coordinate space \mathcal{V} is given by a linearly rising potential $\mathcal{V}(|\vec{x}_q - \vec{x}_{\bar{q}}|) = a + b|\vec{x}_q - \vec{x}_{\bar{q}}|$, in analogy to non-relativistic quark models. We added a residual instanton-induced interaction \mathcal{W} discovered by 't Hooft [7, 8, 2, 3], which acts only on pseudoscalar and scalar mesons and has the form

$$\int d^3 p' [\mathcal{W}(\vec{p}, \vec{p}') \Phi(\vec{p}')] = 4 G \int d^3 p' w_\lambda(\vec{p} - \vec{p}') [1 \text{tr} (\Phi(\vec{p}')) + \gamma^5 \text{tr} (\Phi(\vec{p}') \gamma^5)] \quad (6)$$

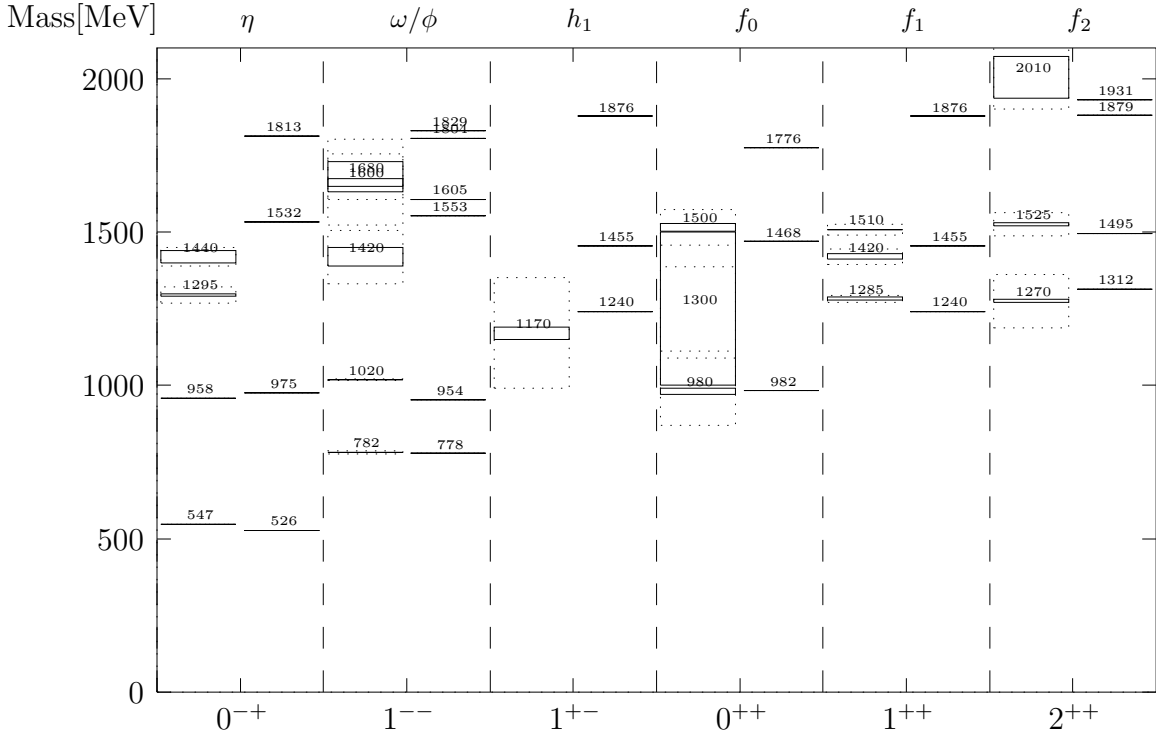


Figure 2: Isoscalar meson spectrum. See also caption to Fig.1.

where $G(g, g')$ is a flavor matrix containing the coupling constants g, g' . Here summation over flavor has been suppressed and w_λ is a regularizing Gaussian function (see [3] for details).

To arrive at a covariant calculation of those transition matrix elements with energy-momentum conservation for both particles, the Bethe-Salpeter amplitude $\chi_P(p)$ depending on the relative four-momentum p has to be known. On the mass shell, it can be reconstructed from the equal time amplitude $\Phi(\vec{p})$: From the Bethe-Salpeter equation the meson-quark-antiquark vertex function $\Gamma_P(p) := [S_1^F(p_1)]^{-1} \chi_P(p) [S_2^F(-p_2)]^{-1}$ is computed in the rest frame from the equal-time amplitude as

$$\Gamma_P(p_{\perp P}) \Big|_{P=(M, \vec{0})} = \Gamma(\vec{p}) = -i \int \frac{d^3 p'}{(2\pi)^4} [V(\vec{p}, \vec{p}') \Phi(\vec{p}')] \quad (7)$$

By a pure boost Λ_P we then can calculate the BS amplitude for any on-shell momentum P of the bound-state by

$$\chi_P(p) = S_{\Lambda_P} \chi_{(M, \vec{0})}(\Lambda_P^{-1} p) S_{\Lambda_P}^{-1}. \quad (8)$$

The Salpeter equation (4) is solved numerically by expanding the Salpeter amplitudes Φ in a finite basis and diagonalization of the resulting RPA- type matrix [4]. Subsequently, the vertex function (7) is reconstructed and used to calculate elektroweak current matrix elements in the Mandelstam formalism, see below and also [9]. The parameters of the model, i.e. the constituent quark masses, m_n, m_s , confinement offset a and slope b were adjusted to the Regge trajectories; the couplings g, g' , and range λ of the instanton induced force were chosen to reproduce the pseudoscalar ground state masses.

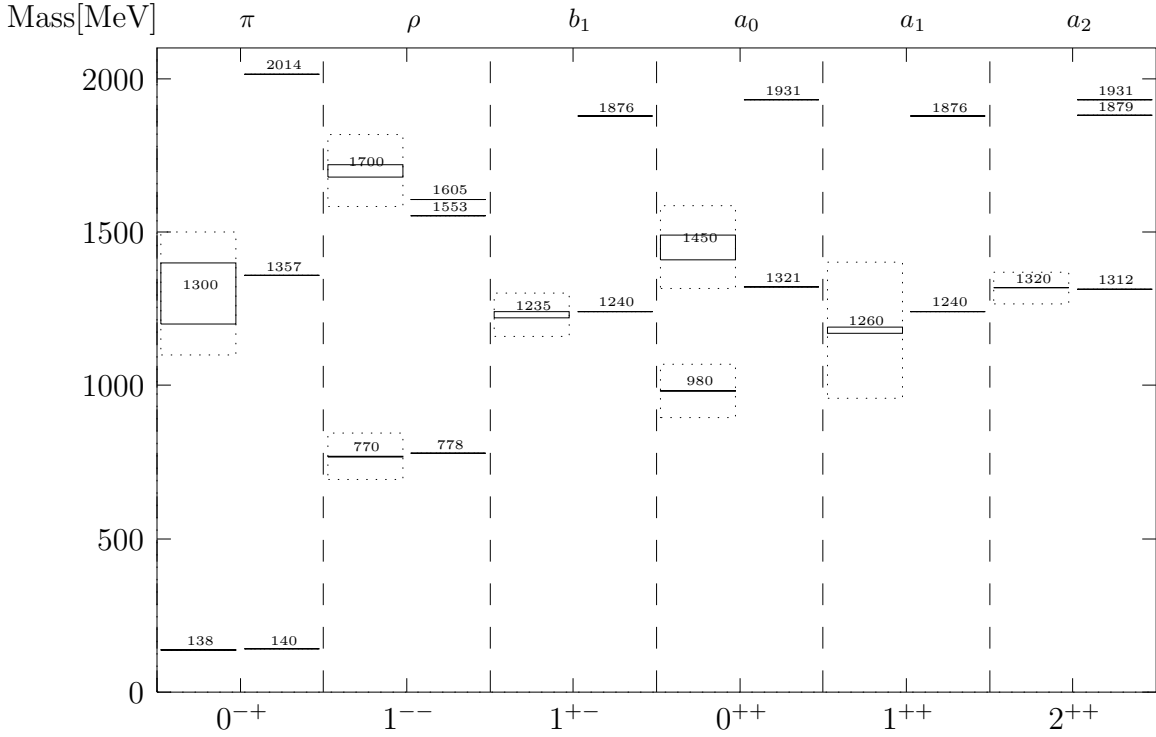


Figure 3: Isovector meson spectrum. See also caption to Fig.1.

3 Spectra and decays of light mesons

The comparison of the experimental and calculated masses of mesons on the Regge trajectories in Table 2 shows, that the present *Ansatz* indeed successfully accounts for the spectra at higher energies. The low energy part of the calculated meson spectra are compared to experimental data in Figs.1–3, for strange, isoscalar and isovector particles, respectively. Note that with the present interaction there are no large spin orbit effects, which is in accordance with experiment for the strange mesons, but certainly does not explain the low lying $a_0(980)$ resonance. We will discuss this and the puzzling situation for the isoscalar, scalar resonances in the following section. The comparison of the experimental and calculated masses of mesons on the Regge trajectories

Table 2: Comparison of experimental [30] and calculated masses (in MeV) of mesons on Regge trajectories.

	exp.	calc.		exp.	calc.		exp.	calc.		exp.	calc.
ω	782	778	ϕ	1020	954	ρ	770	778	K^*	892	870
f_2	1270	1312	f'_2	1525	1495	a_2	1320	1312	K_2^*	1430	1406
ω_3	1670	1698	ϕ_3	1850	1900	ρ_3	1690	1698	K_3^*	1780	1800
f_4	2050	2011	f'_4	2220	2230	a_4	2040	2011	K_4^*	2045	2121
ω_5	2279		ϕ_5	2514		ρ_5	2350	2279	K_5^*	2380	2397
f_6	2510	2517	f'_6	2766		a_6	2450	2517	K_6^*		2642

in Table 2 shows, that the present *Ansatz* indeed successfully accounts for the spectra at higher energies. The low energy part of the calculated meson spectra are compared to experimental data in Figs. 1,1,1, for strange, isovector and isoscalar particles, respectively. Note that with the present interaction there are no large spin orbit effects, which is in accordance with experiment for the strange mesons, but certainly does not explain the low lying $a_0(980)$ resonance. We will discuss this and the puzzling situation for the isoscalar, scalar resonances in the following section.

In order to appreciate the improvement as presented in Table 1 we show in Fig. 4 and 5 the radial part of the Salpeter amplitudes for a deeply bound state like the pion and moderately bound state such as the ρ -meson, respectively. Whereas for the latter the relativistic components are indeed small, and correspondingly the relativistic effects on observables such as given in Table 1 are moderate, for the pion the upper and the lower component of the Salpeter amplitude are of the same size. In the calculation of f_π e.g. essentially their difference enters and hence the correction by an order of magnitude.

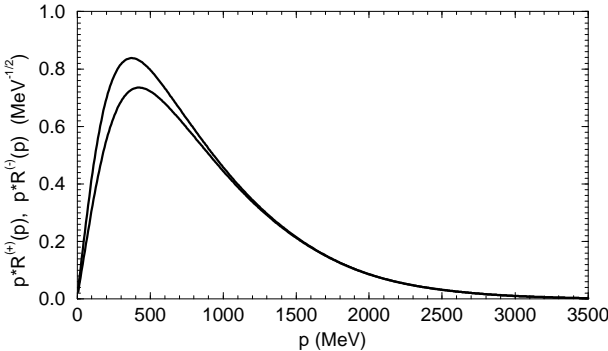


Figure 4: Radial Pion amplitudes $p\mathcal{R}_{00}^{(+)}(p)$ (upper component, upper curve) and $p\mathcal{R}_{00}^{(-)}(p)$ (lower component, lower curve)

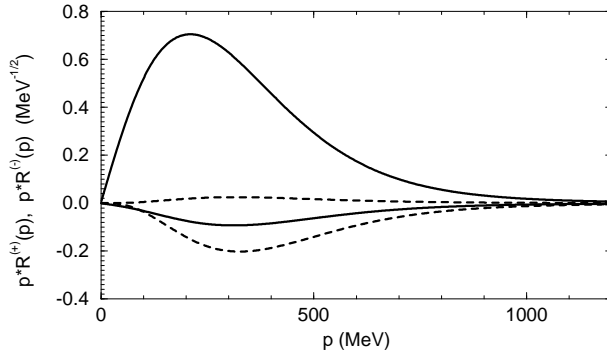


Figure 5: Radial Rho amplitudes $p\mathcal{R}_{01}^{(+)}(p)$ (upper s-wave component, upper solid curve), $p\mathcal{R}_{01}^{(-)}(p)$ (lower s-wave component, lower solid curve), $p\mathcal{R}_{21}^{(+)}(p)$ (upper d-wave component, upper dashed curve), $p\mathcal{R}_{21}^{(-)}(p)$ (lower d-wave component, lower dashed curve)

The general prescription for calculating current matrix elements between bound states has been given by Mandelstam [10], The electromagnetic current operator may be calculated from the BS amplitudes and a kernel $K^{(\gamma)}$ that in its simplest form corresponds to the impulse approximation and reads:

$$K_\mu^{(\gamma)}(P, q, p, p') = -e_1 \gamma_\mu^{(1)} S_2^{F-1}(-P/2 + p) \delta(p' - p + q/2) - e_2 \gamma_\mu^{(2)} S_1^{F-1}(P/2 + p) \delta(p' - p - q/2) \quad (9)$$

where p and p' denote the relative momenta of the incoming and outgoing $q\bar{q}$ pairs, e_1 and $-e_2$ are the charges of the quark and antiquark, $q = P - P'$ is the momentum transfer of the photon.

For the electromagnetic current coupling e.g. to the first quark we have explicitly

$$\begin{aligned} \langle P' | j_\mu^{(1)}(0) | P \rangle &= -e_1 \int \frac{d^4 p}{(2\pi)^4} \\ &\text{tr} \{ \bar{\Gamma}_{P'}((p - q/2)_{\perp P'}) S_1^F(P/2 + p - q) \gamma_\mu S_1^F(P/2 + p) \Gamma_P(p_{\perp P}) S_2^F(-P/2 + p) \} \end{aligned} \quad (10)$$

in terms of the vertex functions Γ , see Eq.(7), given above. We like to point out, that this procedure respects covariance and current conservation for the transitions studied. However, in order to obtain a hermitian current we have to adopt the additional prescription to take only the residue

contributions of the one-particle propagators in the expression above, as otherwise the neglect of retardation effects would yield a anti-hermitian principal-value integral, see also [9].

As an example for electromagnetic observables we compare the calculated $\omega^0 \rightarrow \pi^0$ transition form factor in the space-like region with an extrapolation of the experimental data from the time-like region as measured in dilepton production. It is seen that our results reproduce the vector dominance like behavior of this form factor rather well however without explicitly invoking this mechanism. For other examples of decay widths and form factors, we refer to [9].

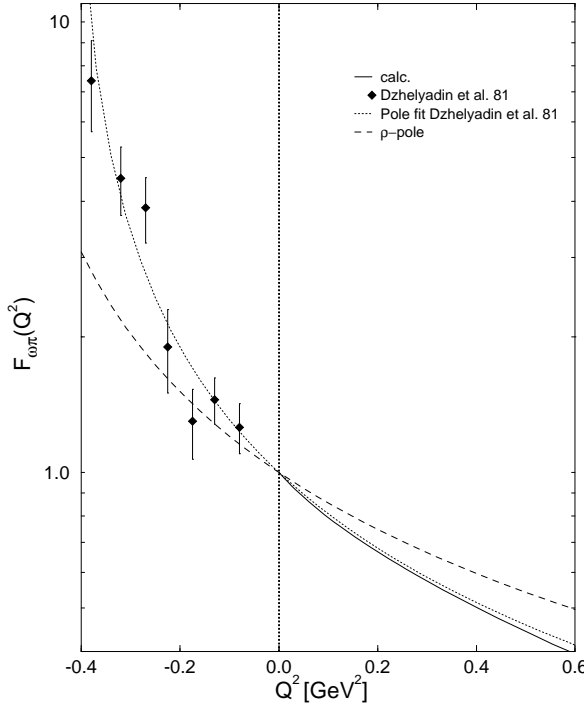


Figure 6: Comparison of the normalized $\omega\pi\gamma^*$ form factor (solid line) in the space-like region with an extrapolation of experimental data in the time-like region [11] (dotted line) and with a ρ -pole *Ansatz* motivated by vector dominance (dashed line)

4 Instanton effects for pseudoscalar and scalar mesons

The flavor dependent effective quark interaction used here was computed by 't Hooft and others from instanton effects [7, 8, 28]. 't Hooft showed that an expansion of the (Euclidean) action around the one instanton solution of the gauge fields with dominance of the zero modes of the fermion fields leads to an effective interaction not covered by perturbative gluon exchange. This interaction is chirally symmetric, see also [14], but breaks the γ_5 - invariance and for three flavors it induces a six-point quark vertex completely antisymmetric in flavor. After normal ordering with respect to the nontrivial QCD vacuum this leads to a contribution to the constituent quarks masses, a two body interaction

$$\Delta\mathcal{L}(2)(y) \propto g_{\text{eff}}^i \varepsilon_{ikl} \varepsilon_{ik'l'} \bar{\Psi}(x) \bar{\Psi}(y) [1 \cdot 1 + \gamma_5 \cdot \gamma_5] (2\mathcal{P}_3^C + \mathcal{P}_6^C) \Psi(x) \Psi(y) \Psi(y) \quad (11)$$

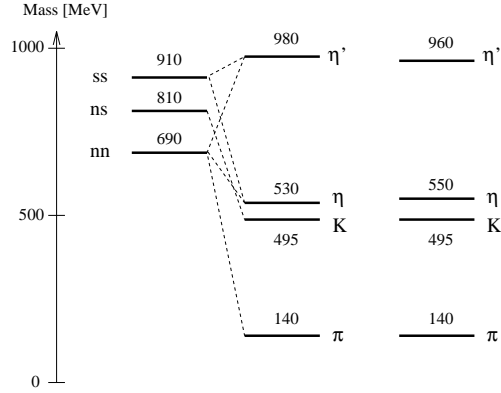


Figure 7: Schematic splitting of the pseudoscalar flavor nonet with confinement interaction (left), with confinement and instanton-induced force (middle) compared to the compilation by the Particle Data Group [30] (right).

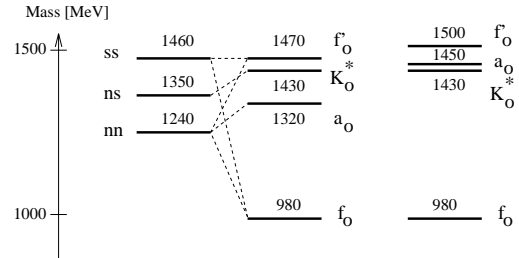


Figure 8: Schematic splitting of the scalar flavor nonet with confinement interaction (left), with confinement and instanton-induced force (middle) compared to the experimental spectrum interpreted as $q\bar{q}$ states [30, 21, 29] (right).

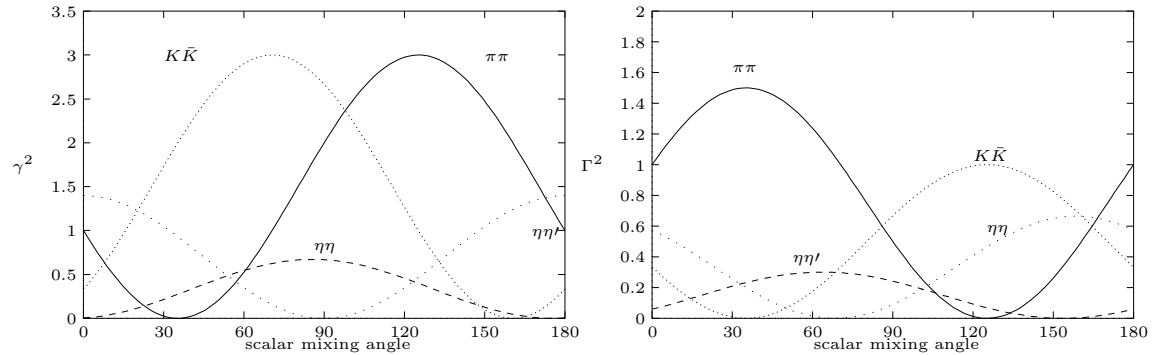


Figure 9: Invariant couplings for the decay of the f'_0 meson into two pseudoscalar mesons: with the conventional OZI rule conserving flavor dependence (left), see also [23], and with the instanton induced three body vertex (right).

and a three body term, see below. Here $i, k, l \in \{u, d, s\}$ are flavor indices, and \mathcal{P}^C are color projectors. This form explicitly shows that this force only acts on antisymmetric flavor states. The spin dependence is such, that this (contact) force acts only for pseudoscalar and scalar mesons. The latter contribution vanishes in the non-relativistic approximation we used in a previous calculation [2], but in the present relativistic model it leads to a sizeable flavor splitting in the scalar spectrum, see Fig. 8, similar to that observed for the π, η, η' pseudoscalars, see Fig. 7, but opposite in sign [3, 12]: In fact, the present model produces an almost pure flavor singlet state f_0^1 at roughly 1 GeV whereas the flavor octet states f_0^8, a_0, K_0^* are almost degenerate close to 1.5 GeV, see Fig. 8, for a treatment in the Nambu, Jona-Lasinio model see [13].

Adopting this prediction then leads to the following interpretation of experimental data as the $q\bar{q}$ -flavor nonet [12]: We propose that the recently discovered $f_0(1500)$, see also [15], is not a glueball but the scalar (mainly)–octet meson for which the $K\bar{K}$ decay mode is suppressed as we will show below. The mainly–singlet state could correspond to the broad $f_0(1000)$ -state introduced by Morgan and Pennington [18, 19], but there are also arguments that it is to be identified with the $f_0(980)$. The isovector and isodoublet states correspond to the $a_0(1450)$ and $K_0^*(1430)$, respectively. Since the spectrum of scalar mesons is rather puzzling [15] some comments are due: The present calculation suggests, that one isoscalar and one isovector scalar state at 1 GeV are not of the quarkonium type. Indeed, coupled channel calculations performed by the Jülich group [17] (but see also [16, 20]) suggest that these resonances are related to $K\bar{K}$ -dynamics. In this spirit, the $f_0(1300)$ resonance is then the high energy part of the broad $f_0(1000)$. For other resonances cited in the literature the evidence is in general not so convincing and will be not discussed here.

However, In particular the $f_0(1500)$ [21] was argued to have properties incompatible with a pure $q\bar{q}$ configuration and was suggested to possess a large glue component [22, 23]. One of the major reasons for this interpretation stems from the decay modes of the $f_0(1500)$ as argued in [22, 23]: There it is found to decay into $\pi\pi$ [24], $\eta\eta$ [25], $\eta\eta'$ [26] but not into $K\bar{K}$ [27]. The $q\bar{q}$ hypothesis cannot fit these branching ratios with a common $SU(3)_f$ scalar mixing angle, when decaying through a conventional decay mechanism (see Fig. 9) obeying Zweig’s rule. Furthermore, the full width $\Gamma(f_0(1500)) = 116 \pm 17$ MeV seems to be incompatible with a nonet structure: Taking the widths $\Gamma(a_0) = 270 \pm 40$ MeV and $\Gamma(K_0^*) = 287 \pm 23$ MeV as a scale for the other members of the scalar nonet, a natural guess for the f_0' width is around 500 MeV. The $f_0(1500)$ thus seems not naturally to fit into the quarkonium nonet. In fact, we will argue, that the same instanton induced forces can yield a decay pattern of the $f_0(1500)$ with a strong $K\bar{K}$ suppression, without assuming a glueball admixture. To this end we invoke the six quark term from the instanton induced interaction which can be written compactly with Weyl spinors $\Psi = (\xi, \eta)$, and spin and color projection operators as (see [32] for details):

$$\Delta\mathcal{L}(3) \propto g_{\text{eff}}^{(3)} \left\{ : \eta^\dagger \eta^\dagger \eta^\dagger \mathcal{P}_1^F (2\mathcal{P}_4^S \otimes \mathcal{P}_{10}^C + 5\mathcal{P}_2^S \otimes \mathcal{P}_8^C) \xi \xi \xi : \right\} + (\eta \longleftrightarrow \xi). \quad (12)$$

Upon calculating the lowest order contribution to the decay amplitude of one meson into two mesons, one finds, that it only acts if (pseudo)scalars are involved and, that the flavor dependence of the instanton induced three-body interaction leads to a selective violation of Zweig’s rule: Only if a flavor singlet participates, there is a contribution, of which the flavor dependence deviates from that of the conventional decay mechanism which obeys Zweig’s rule. Actually this is quite natural, since the substantial splitting and mixing of the pseudoscalar states already indicates that in this sector Zweig’s rule must be violated. This implies, that the empirically very successful OZI-rule, which was the basis of the argument to reject the $f_0(1500)$ as a quarkonium state, can be selectively circumvented in the decays of scalars into pseudoscalars. Indeed Fig. 9 shows quantitatively, that it is indeed possible to account for the peculiar decay pattern of the scalar states, if the $SU(3)$ -mixing in the scalar nonet is small and positive, which is indeed the case in our calculation. In addition this new decay mechanism reduces also the calculated width of f_0^8 , although it is still too large when compared to the experimental value [32].

5 Conclusion

In this contribution we presented the results of a covariant constituent quark model, based on the Bethe-Salpeter equation, and where confinement is implemented by a string like linear potential explaining the Regge trajectories. An instanton induced quark force explains not only the splitting and mixing of pseudoscalar mesons, but suggest that such effects are also present in the spectrum and a violation of the OZI rule in the decays of scalar particles into pseudoscalars. We demonstrated that a covariant treatment that takes into account the relativistic components in the amplitudes is of utmost importance when describing properties of deeply bound states and/or processes at higher momentum transfer. At present we are applying the same concepts in a covariant model of the three-quark system, which is entirely possible but technically rather involved.

6 Acknowledgment

An important part of the material presented here was part of the doctoral theses of C. Münz and J. Resag. We also acknowledge contributions by W. Giersche, S. Hainzl and Ch. Ritter. We highly appreciated the discussions with E. Klempt. Finally the kind hospitality of Prof. L. Jarczyk and his crew in Cracow was very much enjoyed.

References

- [1] UKQCD Collaboration (G.S. Bali et al.), *Phys Lett.* **B309** (1993) 378.
- [2] W. H. Blask, U. Bohn, M. G. Huber, B. C. Metsch, H. R. Petry, *Z. Phys.* **A337** (1990) 327.
- [3] C. R. Münz, J. Resag, B. C. Metsch, H. R. Petry, *Nucl. Phys.* **A578** (1994) 418.
- [4] J. Resag, C. R. Münz, B. C. Metsch, H. R. Petry, *Nucl. Phys.* **A578** (1994) 379.
- [5] E. E. Salpeter, H. A. Bethe, *Phys. Rev.* **84** (1951) 132.
- [6] E. E. Salpeter, *Phys. Rev.* **87** (1952) 328.
- [7] G. 't Hooft, *Phys. Rev.* **D14** (1976) 3432.
- [8] M. A. Shifman, A. I. Vainshtein, V. I. Zakharov, *Nucl. Phys.* **B163** (1980) 46.
- [9] C. R. Münz, J. Resag, B. C. Metsch, H. R. Petry, *Phys. Rev.* **C52** (1995) 2110.
- [10] S. Mandelstam, *Proc. Roy. Soc.* **233** (1955) 248.
- [11] R. I. Dzhelyadin et al., *Phys. Lett.* **B102** (1981) 296.
- [12] E. Klempt, B. C. Metsch, C. R. Münz, H. R. Petry, *Phys. Lett.* **B361** (1995) 160.
- [13] V. Dmitrašinović, *Phys. Rev.* **C53** (1996) 1383.
- [14] M. Nowak, *Chiral symmetry and the matter*, contribution to this workshop.
- [15] H. Koch, *New results on meson spectroscopy with the crystal barrel detector*, contribution to this workshop.
- [16] J. Weinstein, N. Isgur, *Phys. Rev.* **D41** (1990) 2236.
- [17] G. Janssen, B. C. Pierce, K. Holinde, J. Speth, KFA-Jülich preprint KFA-IKP-TH-1994-40, nucl-th/9411021 (1994).

- [18] D. Morgan, M. R. Pennington, Phys. Rev. **D48** (1993) 1185.
- [19] D. Morgan, M. R. Pennington, Phys. Rev. **D48** (1993) 5422.
- [20] N. A. Törnqvist, Helsinki preprint HU-SEFT R 1995-05, hep-ph/9504372 (1995)
- [21] V. V. Anisovitch et al., Phys. Lett. **B323** (1994) 233.
- [22] C. Amsler, F. E. Close, Phys. Lett. **B353** (1995) 385.
- [23] C. Amsler, F. E. Close, Phys. Rev. **D53** (1996) 295.
- [24] D. Alde et al., Phys. Lett. **B201** (1988) 160 and Refs. therein.
- [25] S. Abatzis et al., Phys. Lett. **B324** (1994) 509.
- [26] D. V. Bugg et al., Phys. Lett. **B353** (1995) 378.
- [27] L. Gray et al., Phys. Rev. **D27** (1983) 307.
- [28] H. R. Petry, H. Hofestadt, S. Merk, K. Bleuler, Phys. Lett. **B159**, (1985) 363.
- [29] C. Amsler *et al.*, Phys. Lett. **B294** 451.
- [30] Particle Data Group, Phys. Rev **D50** (1994) 1173.
- [31] C. Amsler et al. (Crystal Barrel Collaboration), Phys. Lett. **B355** (1995) 425.
- [32] Ch. Ritter, B.C. Metsch, C.R. Münz, H.R.Petry, accepted for publication in Phys. Lett. B.